André Weber*

# Testing of solid oxide cells at high current densities

## Test von Festoxid-Zellen bei hohen Stromdichten

https://doi.org/10.1515/teme-2021-0102
Received September 25, 2021; accepted November 9, 2021

**Abstract:** Solid Oxide Cells (SOCs) have gained an increasing interest as electrochemical energy converters due to their high efficiency, fuel flexibility and ability of reversible fuel cell/electrolysis operation. During the development process as well as in quality assurance tests, the performance of single cells and cell stacks is commonly evaluated by means of current/voltage- (CV-) characteristics. Despite of the fact that the measurement of a CV-characteristic seems to be simple compared to more complex, dynamic methods as electrochemical impedance spectroscopy or current interrupt techniques, the resulting performance strongly depends on the test setup and the chosen operating conditions.

In this paper, the impact of different single cell testing environments and operating conditions on the CV-characteristic of high performance cells is discussed. The influence of cell size, contacting and current collection, contact pressure, fuel flow rate and composition on the achievable cell performance is presented and limitations arising from the test bed and testing conditions will be pointed out. As today's high performance cells are capable of delivering current densities of several ampere per $cm^2$ a special emphasis will be laid on single cell testing in this current range.

**Keywords:** Fuel cell, solid oxide cell, SOC, current/voltage-characteristic, contact resistance, fuel utilization.

**Zusammenfassung:** Festoxidzellen (Solid Oxide Cells, SOCs) haben aufgrund ihres hohen Wirkungsgrads, ihrer Brennstoffflexibilität und ihrer Fähigkeit zum reversiblen Brennstoffzellen/Elektrolyse-Betrieb als elektrochemische Energiewandler zunehmend an Interesse gewonnen. In der Entwicklung wie auch zur Qualitätssicherung wird die Leistung von Einzelzellen und Zellstacks in der Regel anhand von Strom/Spannungs-Kennlinien bewertet. Obwohl die Messung einer Strom/Spannungs-Kennlinie im Vergleich zu komplexeren, dynamischen Methoden wie der elektrochemischen Impedanzspektroskopie oder Current-Interrupt Techniken einfach zu sein scheint, hängt die resultierende Leistung stark vom Testaufbau und den gewählten Betriebsbedingungen ab.

In diesem Beitrag werden die Auswirkungen verschiedener Testumgebungen und Betriebsbedingungen auf die Kennlinie leistungsfähiger Festoxidzellen diskutiert. Der Einfluss von Zellgröße, Kontaktierung und Stromableitung, des Kontaktdrucks, der Brenngasausnutzung und der Brenngaszusammensetzung auf die erreichbare Zellleistung wird dargestellt. Einschränkungen durch den Prüfstand und die Prüfbedingungen werden diskutiert. Da die heutigen Hochleistungszellen in der Lage sind, Stromdichten von mehreren Ampere pro $cm^2$ zu liefern, wird ein besonderer Schwerpunkt auf die Einzelzellenprüfung in diesem Strombereich gelegt.

**Schlagwörter:** Brennstoffzelle, Festoxidzelle, Strom/Spannungs-Kennlinie, Kontaktwiderstand, Brenngasausnutzung.

## 1 Introduction

Solid oxide cells enable high power densities in the fuel cell (SOFC) and electrolyzer mode (SOEC). The cells consist of a porous fuel electrode, a dense oxygen-ion conductive ceramic electrolyte and a porous air electrode. There are differences with regard to the mechanical support, e. g. electrolyte supported cells exhibiting a 50 to 200 µm thick electrolyte substrate and electrode supported cells, mostly supported by a 200 to 500 µm thick, porous Ni/YSZ[1]-layer at the fuel electrode side. Due to operating temperatures in the range from 500 to 1000 °C SOCs are capable of converting different available fuels as hydrogen, natural gas, propane, biogas etc. into electrical energy and vice versa – preferably regenerative – electrical energy into chemical energy carriers as hydrogen, syngas or carbon monoxide.

***Corresponding author: André Weber,** Karlsruhe Institute of Technology (KIT), Institute for Applied Materials (IAM-ET), Adenauerring 20b, 76131 Karlsruhe, Germany, e-mail: andre.weber@kit.edu, URL: http://www.iam.kit.edu/et/english/mitarbeiter_andre_weber.php

1 YSZ: yttria stabilized zirconia.

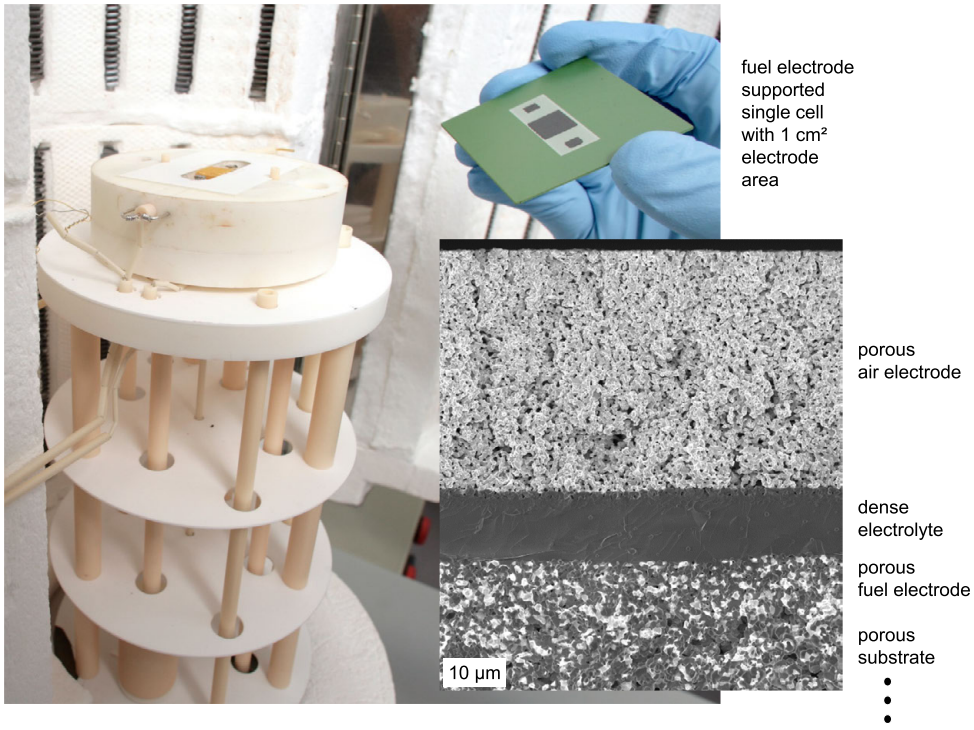


**Figure 1:** Housing and gas tubing in the furnace of a single cell test bench, fuel electrode supported single cell with a 1 $cm^2$ air electrode and scanning electron microscopy image of the cell displaying a cross section within the active cell area.

The ability of reversible SOFC/SOEC-operation offers significant advantages considering energy storage on larger scales that will be mandatory for the energy transition.

As the open circuit voltage (OCV) of a cell is in the range of 1 V only, technical applications of SOCs require a serial connection of a sufficient number of cells (20 to >100) in a stack in order to achieve technically meaningful voltage levels. For performance analysis and detailed electrochemical characterization of SOCs, single cell tests in specially designed cell housings mounted in a test bench are performed. This approach is mandatory for cell and electrode development, quality assurance in cell production, studies of intrinsic degradation phenomena and a reliable comparison of cells from different manufacturers. Single cell test are applied before a new material, electrode or type of cell is integrated in a stack or even system. This ensures that the cell reaches the required performance and durability. A general advantage of single cell testing is the elimination of impacts related to the stack i. e. its flowfields, the contacting geometry and related contact resistances as well as poisoning effects resulting from sealing materials or corrosion products of metallic interconnectors. Furthermore development costs can be reduced drastically as inadequate cells can be rejected in an early development stage without the costly integrating into a stack. In case of solid oxide cells a testing environment based on inert materials is preferably used. The housing components are commonly made of chemically inert and insulating materials as aluminum oxide ($Al_2O_3$) that are neither affected by high operating temperatures of up to 1000 °C nor by the oxidative or reductive gas composition of the oxidant or fuel respectively. Noble metals (Pt, Au) are often applied as contact elements and current collectors. They are mandatory for the oxidative conditions at the air electrode, whereas cheaper materials as nickel are applicable for contacting the fuel electrode. Preferably a contacting via meshes is applied as the highly porous and flexible mesh structure ensures a homogeneous contacting and current collection all over the active electrode area and simultaneously a sufficient gas supply to the electrode surface. In SOC-stacks these advantages can only be reused on the fuel electrode side by integrating a Ni-mesh in-between electrode and interconnector. The noble metal grids applied in single cell tests on the air electrode are by far too expensive as a contact layer in commercial SOFC-stacks. Thus on the stack and system level other solutions as ceramic contact pastes are applied despite of the associated challenges and limitations. As a result, the performance of a single cell test often exceeds the performance of the identical cell in a stack.

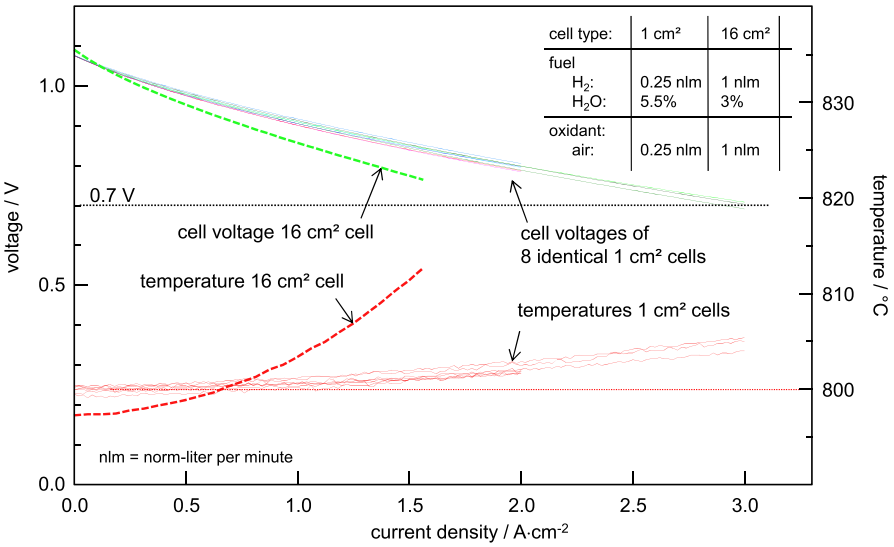


**Figure 2:** CV-characteristics of nominally identical cells in SOFC mode exhibiting different active electrode areas of 1 and 16 $cm^2$ respectively. The temperature is measured by thermocouples close to the cell (distance < 2 mm).

In many previous studies the performance of single cells, exhibiting an active cell area in the range of 0.25 to 16 $cm^2$, was determined using slightly humidified hydrogen (~ 3 % $H_2O$) as the fuel and air or oxygen as the oxidant. In case of small electrode areas and high gas flow rates the gas utilization in these single cell tests is usually quite small (≪50 %) and thus far away from technically meaningful values exceeding a fuel utilization of at least of 70 %.

Applying such testing conditions to high performance fuel electrode supported SOC's, which is mandatory to be able to compare their performance with former cell generations, will result in much higher current density values exceeding 1 A/$cm^2$ significantly. Under these conditions additional losses related to in-plane ohmic losses in the current collector, the contact resistance in between current collector and electrode as well as gas diffusion in the substrate and gas conversion along the gas channel will impact the cell performance.

The aim of this contribution is to illustrate the impact of the design of the test setup and the chosen testing conditions on the evaluated performance of single cells. A special emphasis is laid on single cell testing at high current densities.

# 2 Experimental results

The cell tests described in this paper were mostly performed on fuel electrode supported solid oxide fuel cells, exhibiting a Ni/YSZ substrate, a Ni/YSZ fuel electrode, an 8YSZ electrolyte, a CGO barrier layer and a LSCF-air electrode. Details regarding the cell design and manufacturing procedures can be found in [1, 2]. The electrochemical properties of the cells are described in [3, 4] and approaches for cell performance modeling including large sized cells and stacks are outlined in [5, 6, 7, 8]. Detailed information regarding the test benches and testing procedures can be found in [9, 10].

## 2.1 Cell size

Cells with 1 $cm^2$ and 16 $cm^2$ active electrode area have been analyzed in SOFC mode. A comparison of the performance evaluated for identical cells exhibiting 1 $cm^2$ and 16 $cm^2$ active electrode areas respectively is given in Figure 2.

It is obvious, that the 1 $cm^2$ cells show an excellent reproducibility in both current voltage and temperature behavior but, despite of the similar cell configuration, a higher performance in comparison with the 16 $cm^2$ cell. In general such differences have to be attributed to 3 main reasons:

– The risk of a partly insufficient contacting increases with the size of the active electrode. Especially in case of an inhomogeneous thickness or a warpage of the cell, severe contacting problems might arise. As flat cells with a constant thickness have been applied in this study an inhomogeneous contacting can be excluded.

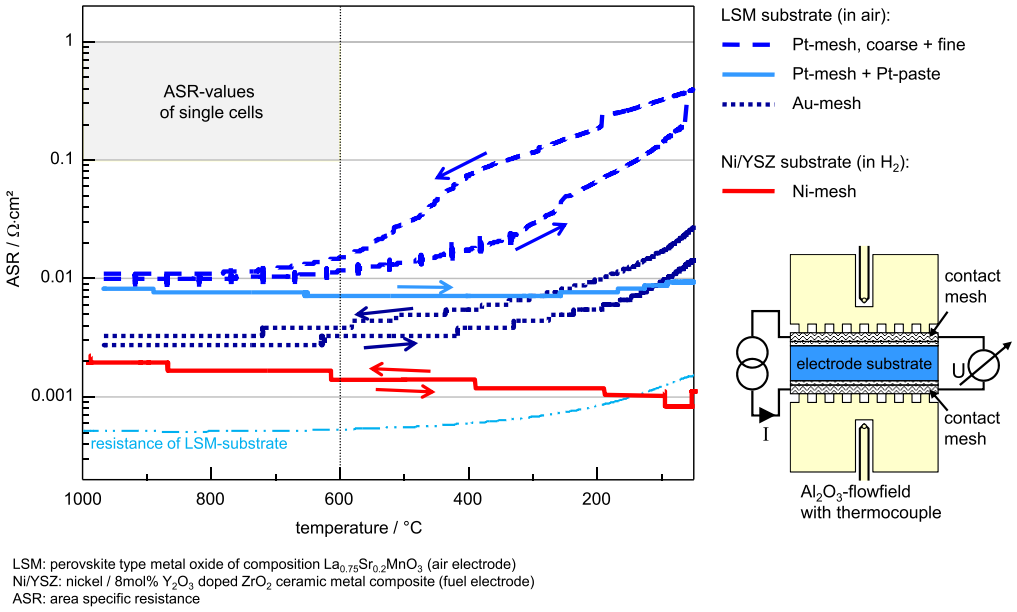


LSM: perovskite type metal oxide of composition $La_{0.75}Sr_{0.2}MnO_3$ (air electrode)
Ni/YSZ: nickel / 8mol% $Y_2O_3$ doped $ZrO_2$ ceramic metal composite (fuel electrode)
ASR: area specific resistance

**Figure 3:** Contact resistance of different meshes for electrode contacting: Pt and Au for the air electrode and Ni for the fuel electrode. The apparent hysteresis is related to an improved contacting at elevated temperatures.

- In case of thin electrode layers and current collectors with a high in-plane resistance the related ohmic losses will decrease the cell performance. This decrease increases with the active cell area.
- Cells exhibiting a larger active cell area are often operated at higher fuel utilization. In Figure 2 the electrode area is increased by a factor of 16 whereas the gas flow is only increased by a factor of 4. The impact of fuel gas utilization can be considered by an appropriate model as described in [11].

## 2.2 Contacting and current collection

In many single cell tests an apparently ideal contacting and current collection is realized by metallic contact meshes exhibiting a high conductivity. In a previous study [12] we have analyzed the contact resistance between the porous electrode materials (e. g. Ni/YSZ- and LSM-substrates) and different current collectors (Figure 3). It was shown that gold meshes are ideal for the air electrode whereas Ni-meshes should be applied at the fuel electrode. Furthermore the use of contact pastes (platinum, silver etc.), not applicable in stacks, should be avoided as they will affect the cell performance. The contact pressure respectively weight applied onto the active electrode area was varied in between 40 and 500 gr/cm$^2$. For the cells investigated in this study it was found that a contact weight of 100 gr/cm$^2$ is sufficient, nevertheless the cells exhibiting an active electrode area of 16 cm$^2$ (Figure 2) were loaded with a contact weight of 4 kg corresponding to 250 gr/cm$^2$.

Next to the contact resistance between electrode and current collector the in-plane resistance of the current collecting layers has to be considered. The in-plane resistance of a conductive layer $R_{ip}$ is depending on the conductivity of the material $\sigma$ and the thickness of the layer $d$.

$$R_{ip} = \frac{1}{\sigma \cdot d} \tag{1}$$

It should be noted that despite of its unit "Ω" it is a layer specific value that cannot directly be applied in Ohm's law. The voltage losses $V$ due to an in-plane current $I$ in a layer with a width $W$ (perpendicular to the direction of the current) and a length $L$ (in the direction of the current) can be calculated according to Equation (2):

$$V = R_{ip} \cdot \frac{L}{W} \cdot I \tag{2}$$

In Table 1 the in-plane resistance for electrodes and different current collectors is displayed as a function of temperature. A comparison of the in-plane resistances shows that the value for the air electrode is significantly higher than all other in-plane resistance values, even if a rather thick (100 µm) air electrode based on a highly conductive metal oxide (LSC: $La_{0.6}Sr_{0.4}CoO_3$) would be applied. In case of other air electrode materials exhibiting a much lower conductivity (LSCF, LSM) the in-plane resistance will be even higher.

**Table 1:** Properties and resulting in-plane resistance of different current collectors.

| electrodes | thickness | material ratio | tortuosity | effective layer thickness | bulk conductivity | in-plane resistance |
|---|---|---|---|---|---|---|
| Ni/YSZ-substrate | 500 µm | 26 % | 2.1 | 61 µm | 12400 S/m | 0.0133 Ω |
| LSC-electrode | 100 µm | 60 % | 2.0 | 30 µm | 1449 S/m | 0.2301 Ω |
| **current collector** | **wire ⌀** | **mesh** | **wires** | | | |
| Au mesh fine | 60 µm | 1024 $cm^{-2}$ | 32.0 $cm^{-1}$ | 9 µm | 104000 S/m | 0.0106 Ω |
| Au mesh coarse | 250 µm | 100 $cm^{-2}$ | 10.0 $cm^{-1}$ | 49 µm | 104000 S/m | 0.0020 Ω |
| Au wires | 500 µm | | 3.8 $cm^{-1}$ | 74 µm | 104000 S/m | 0.0013 Ω |
| Ni mesh fine | 80 µm | 2304 $cm^{-2}$ | 48.0 $cm^{-1}$ | 24 µm | 12400 S/m | 0.0334 Ω |
| Ni mesh coarse | 1500 µm | 900 $cm^{-2}$ | 30.0 $cm^{-1}$ | 53 µm | 12400 S/m | 0.0152 Ω |
| Ni wires | 500 µm | | 3.8 $cm^{-1}$ | 74 µm | 12400 S/m | 0.0110 Ω |
| Ni flowfield | d = 2 mm | solid material | – | 1500 µm | 12400 S/m | 0.0005 Ω |

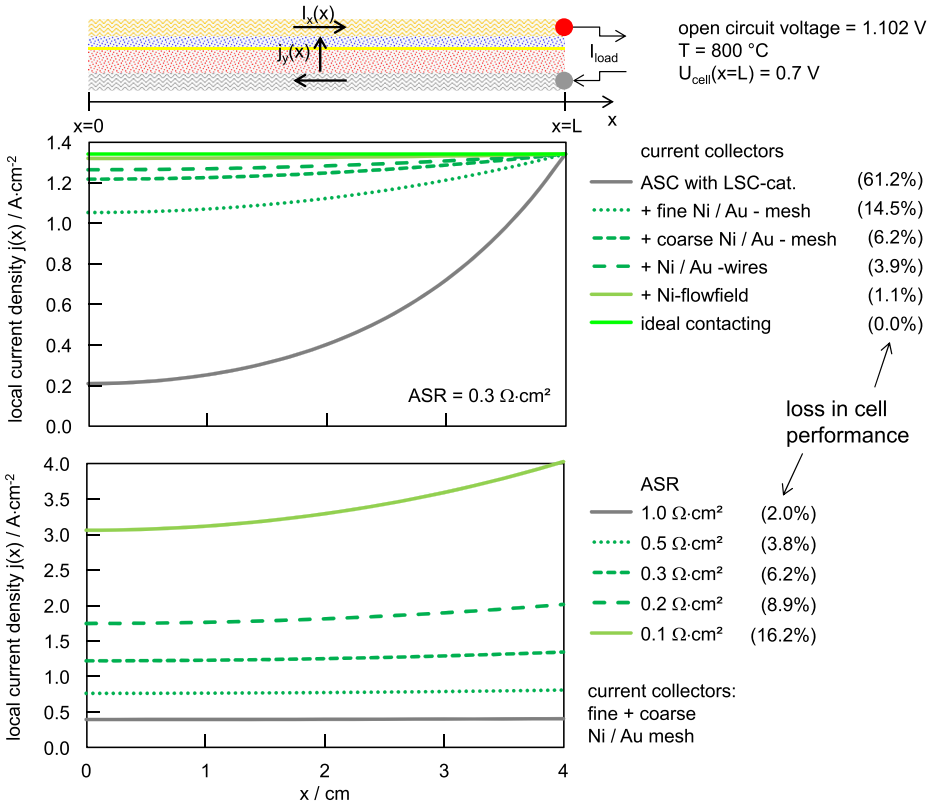


**Figure 4:** Current density distribution in a 16 $cm^2$ single cell (4 cm × 4 cm) for different combinations of current collectors (top) and cells differing in ASR (bottom). The current $I_{load}$ is supplied at x = L. The values in brackets correspond to the loss in power density due to the current collectors. The power density was calculated by multiplying the average current density with the voltage $V_{cell}(x = L) = 0.7\,V$. The performance achieveable for an ideal contacting was used as the reference value (100 %).

Applying a simple analytical 2D SOFC model (see Appendix A) and assuming a cell that exhibits a constant area specific resistance (ASR) as well as a constant gas composition all over the active cell area, the current density distribution arising from an insufficient in-plane resistance of electrodes and current collectors can be estimated.

In Figure 4 the results for a 16 $cm^2$ single cell are displayed for different combinations of current collectors (top) and cells differing in ASR (bottom). It is obvious, that the cell without any metallic current collectors (current collection performed by the substrate and a 100 µm thick, porous LSC-air electrode) will show a significant performance decrease[2] of 61 % as the current density in large areas of the cell is limited by the in-plane losses in the elec-

**2** The apparent cell performance depends on the positioning of the voltage probes. The local cell voltage $V_{cell}(x)$ (see Appendix A) will be measured, which is increasing with decreasing x.

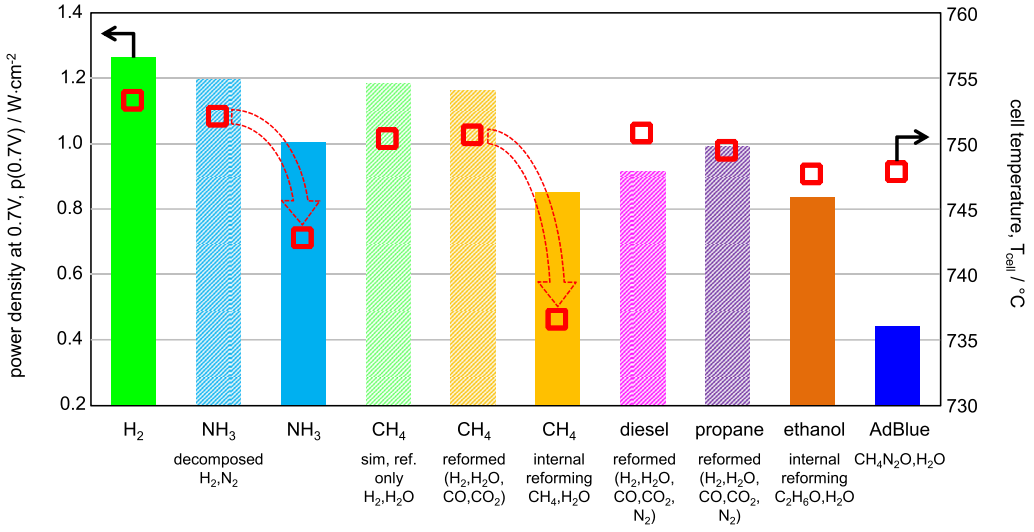


**Figure 5:** Cell performance (power density at 0.7 V cell voltage) of identical 1 $cm^2$ single cells achieved with different fuels. In case of fuels catalytically converted in an endothermal reaction (ammonia decomposition, internal reforming of methane), the resulting reduction in cell temperature decreases the achievable power density.

trodes. By decreasing the in-plane resistance of the current collectors by applying appropriate combinations of contact meshes and wires the performance decrease can be reduced to values in the range of a few %.

In order to minimize performance losses related to an insufficient current collection at 16 $cm^2$ cells, in this study a combination of fine and coarse gold mesh onto which 0.5 mm ⌀ gold wires were welded has been used as the air electrode current collector whereas a metallic flowfield and appropriate Ni-meshes were applied at the fuel electrode. In addition the electrical current was supplied on both sides of the current collector. Therefore negligible performance losses fairly below 1 % can be expected.

## 2.3 Impact of fuel composition

Solid oxide fuel cells exhibit a high fuel flexibility and therefore can be operated with various fuels and reformates thereof respectively [13]. In addition to hydrogen, carbon monoxide and methane as well as ammonia and similar species can be converted directly in the cell. In most cases this fuel conversion takes place by a preceding catalytic reaction generating hydrogen, i. e. the water-gas shift reaction, the internal reforming of methane or the decomposition of ammonia, followed by the electrooxidation of the generated hydrogen in an electrochemical reaction [14]. In case of fuels containing higher hydrocarbons as propane or diesel, the catalytic conversion can hardly be performed in the cell [15]. An external reformer unit is mandatory in order to achieve a complete fuel conversion and to avoid the formation of soot and carbon deposits in the cell. In case of a stable fuel supply that is not affecting the integrity of the cell, the achievable cell performance depends on the hydrogen concentration and can furthermore be affected by a temperature decrease due to endothermal catalytic reactions. In Figure 5 the effect of different fuel compositions on the power density and the operating temperature is displayed.

With respect to single cell testing, (humidified) hydrogen is the most common fuel, as it can be directly fed to the cell and no fuel processing in the test bench is required. The application of hydrogen in single cell tests is useful for the rating of different materials, electrodes or cells, but does not provide information about the cell performance and durability to be expected with other fuels.

## 2.4 Impact of fuel flow rate

Next to the fuel composition, the fuel gas flow rates and the corresponding gas utilizations influence the evaluated cell performance. In Figure 6 current/voltage-characteristics of a fuel electrode supported cell operated at different fuel flow rates are displayed. It is visible that the OCV as well as cell performance (current density at 0.7 V cell voltage) show a significant dependency on the fuel gas flow rate.

The measured OCV is affected by the leakage (and the oxygen content of the supplied fuel) [9]. In case of dry hydrogen exhibiting nearly no oxygen or water the oxygen

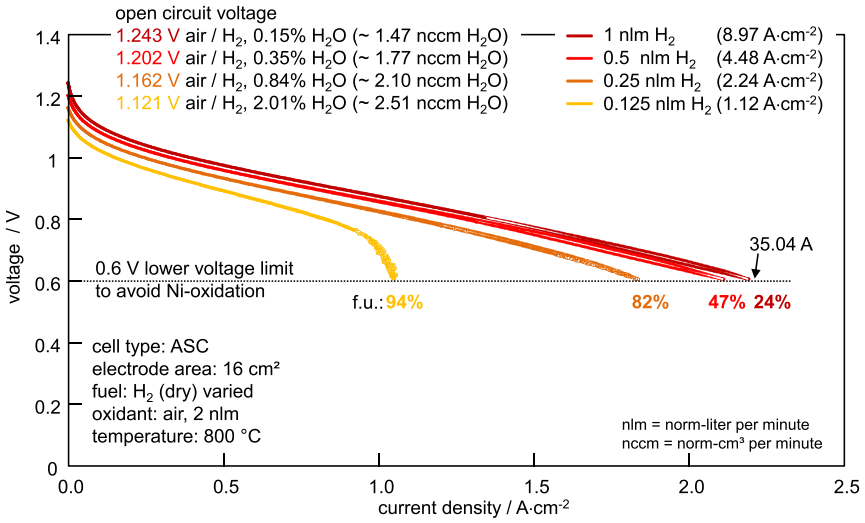


**Figure 6:** Current/voltage-characteristics of an ASC measured at different fuel gas flow rates.

leakage into the fuel compartment can be calculated by the Nernst-equation. For the given setup the water vapor content in the fuel varies in between 0.15 % and 2 % corresponding to an oxygen leakage of 0.73 to 1.26 sccm $O_2$ diffusing into the fuel compartment. The strong variation in OCV is related to the low water vapor content of the supplied fuel. In case of humidified hydrogen the impact of the fuel flow rate on the OCV is significantly reduced.

The cell performance is influenced by the fuel gas flow rate in two different ways. In case of an insufficient fuel gas supply (here at 0.125 slm $H_2$) the current is limited by the available amount of fuel. Such gas conversion limitation usually becomes visible at a fuel utilization (f. u.) exceeding 80 %. By increasing the fuel flow rate by a factor of 2, a significant increase in cell performance at 0.6 V cell voltage of factor 1.74 is observed. Further doubling of the fuel flow rates to 0.5 and 1.0 slm $H_2$ only results in a minor performance increases of 15 % and 3.8 % respectively. Under these conditions it is no longer the available amount of fuel gas but the different losses in the cell that are limiting the cell performance.

If mass transport in the cell is sufficiently fast, the limiting current density related to fuel conversion will be observed at fuel utilizations exceeding 80 %. In case of a gas diffusion limitation in the porous electrodes a quite similar shape of the CV-characteristic can also be observed at much lower fuel utilization.

## 2.5 Impact of temperature measurement

Usually the temperature of the tested single cell is measured by a thermocouple, which should be placed as close as possible to the cell. We have shown that the temperature measured by a thermocouple placed just 1 mm underneath a small sized (1 $cm^2$) cell still undercuts the electrolyte temperature, which was evaluated by the temperature dependency of the high frequency part of the impedance spectra [11]. In the SOFC mode the "cell temperature" measured by a thermocouple is usually below the real cell temperature. In case of SOEC operation a temperature decrease due to the endothermic reactions results in a lower cell temperature [12]. The same holds for catalytic reactions as steam reforming [13]. From Figure 2 it is obvious, that in case of larger active cell areas the increase in cell temperature with increasing current density is even more pronounced. Figure 7 reveals the temperatures measured in a single cell test during a CV-characteristic. Next to the furnace temperature $T_{furnace}$, which mostly deviates significantly from the cell temperature, the temperature of the cell housing $T_{housing}$ and the temperatures along a gas channel $T_{gc}$ [16] (~ 1 mm beneath the cell) are measured. In this case the temperature gradient along the gas channel is rather small, which has to be attributed to the Ni-flowfield that exhibits not only a very high electrical but also a very high thermal conductivity. It is also obvious that the temperature measured "somewhere" in or at the housing (in this example ~ 1 cm away from the cell resulting in an approximately 12 K lower temperature) is no useful value.

Furthermore there is a significant temperature increase visible, which is related to the voltage losses increasing with the current density. To evaluate the cell performance at a desired temperature such temperature increase has to be taken into account and an appropriate furnace temperature has to be selected.

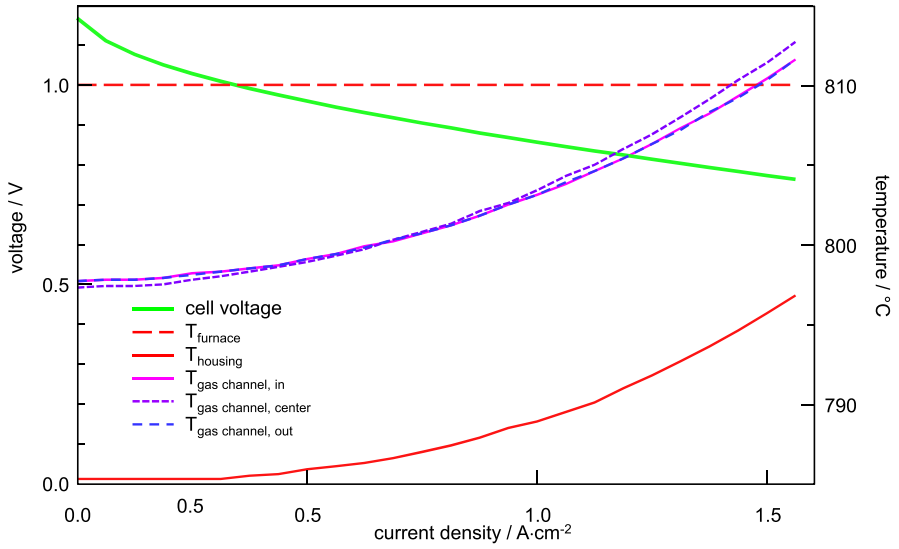


**Figure 7:** Temperatures measured by thermocouples at different locations during a CV-characteristic measurement.

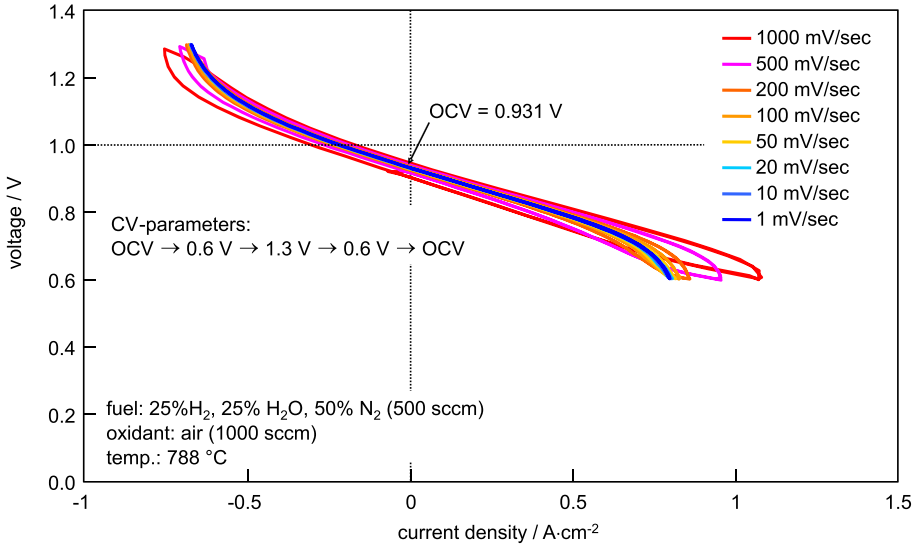


**Figure 8:** CV-characteristics measured with different slew rates. Here the potentiostatic mode was selected in the measurement to avoid cell voltages below 0.6 V/above 1.3 V that might damage the cell.

## 2.6 Impact of CV-characteristic parameters

There is a number of parameters influencing the shape of a CV-characteristic and hence the evaluated cell performance. Slew rate, step size and holding time at each current value can influence the result. An example is given in Figure 8. CV-characteristics in SOFC and SOEC mode of one single cell measured under identical operating conditions but differing in the slew rate show significant differences.

In case of very fast slew rates the “slow” loss mechanisms as gas diffusion are only partly activated. The required reactants, which have to be provided from the gas channel by diffusion through the substrate under steady state conditions, can be taken from the pore volume as long as the total measuring time is in the range of one second. The observed hysteresis is related to a depletion of this gas phase capacity.

In case of slower slew rates the onset of the gas diffusion limitation is shifted to lower current densities. Thus the hysteresis is reduced. The performance is on the one hand reduced, as the gas diffusion polarization contributes to the voltage losses in the cell, on the other hand the increase in temperature enhances the performance.

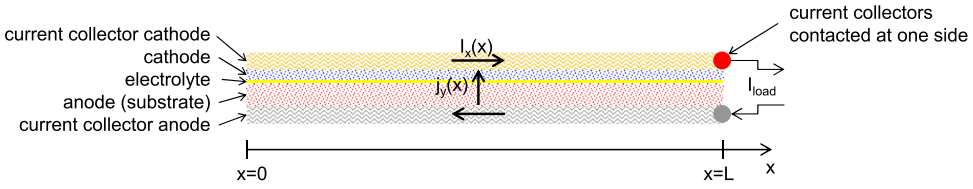


**Figure 9:** Sketch of the contacted cell.

# 3 Summary

For the characterization of high performance solid oxide single cells at high current densities the selection of an appropriate test bench design and appropriate testing conditions is crucial. To avoid erroneous results related to contacting, gas supply and temperature measurement a number of measures have to be considered.

- Current collectors with a sufficiently low in-plane resistance as well as a negligible contact resistance should be selected.
- Appropriate gas compositions and gas flow rates should be selected. A performance limitation by the amount of fuel gas (or oxygen) supplied to the cell should be avoided.
- The cell temperature should be measured at a location close to the active electrode area. The temperature increase occurring during imposing of electrical current on the cell should be considered in the data analysis.
- Parameters for a CV-characteristic measurement should be selected carefully.

It should always be taken into account, that the apparent performance of a single cell evaluated by means of CV-characteristics can be “adjusted” in a wide range if the operator is aware of those interrelationships.

# Appendix A

in-plane current:

$$I_x(x) = b \cdot \int_0^x j_y(u)du \tag{A1}$$

b: width of the cell
local cell voltage:

$$V_{cell}(x) = OCV - ASR \cdot j_y(x) \tag{A2}$$

cell voltage at x = L:

$$V_{cell}(L) = OCV - \frac{R_{ip}}{b} \cdot \int_x^L I_x(u)du - ASR \cdot j_y(x) \tag{A3}$$

in-plane resistance:

$$R_{ip} = R_{ip,cathode} + R_{ip,anode} \tag{A4}$$

local current density:

$$j_y(x) = \frac{1}{ASR} \cdot (OCV - V_{cell}(L) - \frac{R_{ip}}{b} \cdot \int_x^L I_x(u)du) \tag{A5}$$

combining (A1) and (A6):

$$I_x(x) = \frac{b}{ASR} \cdot \int_0^x (OCV - V_{cell}(L) - \frac{R_{ip}}{b} \cdot \int_v^L I_x(u)du)dv \tag{A6}$$

$$I_x(x) = \frac{b \cdot (OCV - V_{cell}(L))}{ASR} \cdot x - \frac{R_{ip}}{ASR} \cdot \int_0^x \left( \int_v^L I_x(u)du \right) dv \tag{A7}$$

differential equation:

$$\frac{\partial^2 I_x(x)}{\partial x^2} = k^2 \cdot I_x(x) \quad \text{with } k^2 = \frac{R_{ip}}{ASR} \tag{A8}$$

solution:

$$I_x(x) = \alpha \cdot sinh\,(k \cdot x) \tag{A9}$$

$$\text{with } \alpha = (OCV - V_{cell}(L)) \cdot b \cdot \sqrt{\frac{1}{ASR \cdot R_{ip}}} \cdot \frac{1}{\cosh\,(k \cdot L)}$$

local current density:

$$j_y(x) = \frac{OCV - V_{cell}(L)}{ASR} \cdot \frac{\cosh\,(k \cdot x)}{\cosh\,(k \cdot L)} \tag{A10}$$

local cell voltage:

$$V_{cell}(x) = OCV - (OCV - V_{cell}(L)) \cdot \frac{\cosh\,(k \cdot x)}{\cosh\,(k \cdot L)} \tag{A11}$$

# References

1. D. Stöver, H. P. Buchkremer, F. Tietz and N. H. Menzler, Trends in Processing of SOFC Components, In: (J. Huijsmans, ed), Proceedings of the 5th European Solid Oxide Fuel Cell Forum, pp. 1–9, 2002.

2. N. Menzler, W. Schafbauer, F. Han, O. Büchler, R. Mücke, H. P. Buchkremer and D. Stöver, Development of High Power Density Solid Oxide Fuel Cells for long-term operation, Materials Science Forum 654–656, pp. 2875–2878, 2010.
3. A. Leonide, V. Sonn, A. Weber and E. Ivers-Tiffée, Evaluation and modeling of the cell resistance in anode-supported solid oxide fuel cells, J. Electrochem. Soc. 155, pp. B36–B41, 2008.
4. C. Endler, A. Leonide, A. Weber, F. Tietz and E. Ivers-Tiffée, Time-Dependent Electrode Performance Changes in Intermediate Temperature Solid Oxide Fuel Cells, J. Electrochem. Soc. 157, pp. B292–B298, 2010.
5. A. Leonide, S. Hansmann and E. Ivers-Tiffée, A 0-Dimensional Stationary Model for Anode-Supported Solid Oxide Fuel Cells, ECS Trans. 28, pp. 341–346, 2010.
6. D. Klotz, A. Leonide, A. Weber and E. Ivers-Tiffée, Electrochemical model for SOFC and SOEC mode predicting performance and efficiency, International Journal of Hydrogen Energy 39, pp. 20844–20849, 2014.
7. D. Klotz, A. Weber and E. Ivers-Tiffée, Dynamic Electrochemical Model for SOFC-Stacks, ECS Trans. 25, pp. 1331–1340, 2009.
8. D. Klotz, J. P. Schmidt, A. Weber and E. Ivers-Tiffée, Performance model for large area solid oxide fuel cells, J. Power Sources 259, pp. 65–75, 2014.
9. A. Weber, A. C. Müller, D. Herbstritt and E. Ivers-Tiffée, Characterization of SOFC Single Cells, In: (H. Yokokawa and S. C. Singhal, eds), Proceedings of the 7th International Symposium on Solid Oxide Fuel Cells, pp. 952–962, 2001.
10. D. Klotz, A. Weber and E. Ivers-Tiffée, Practical Guidelines for Reliable Electrochemical Characterization of Solid Oxide Fuel Cells, Electrochim Acta 227, pp. 110–126, 2017.
11. D. Klotz, A. Weber and E. Ivers-Tiffée, Thermal Behavior of SOFC Single Cells in Operation with Dynamic Loads, In: (R. Steinberger-Wilckens and U. Bossel, eds), Proceedings of the 8th European Solid Oxide Fuel Cell Forum, p. B0909, 2008.
12. J.-C. Njodzefon, D. Klotz, A. Kromp, A. Weber and E. Ivers-Tiffée, Electrochemical Modeling of the Current-Voltage Characteristics of an SOFC in Fuel Cell and Electrolyzer Operation Modes, J. Electrochem. Soc. 160, pp. F313–F323, 2013.
13. A. Weber, Fuel flexibility of solid oxide fuel cells, Fuel Cells, 2021. Doi: 10.1002/fuce.202100037.
14. A. Kromp, A. Leonide, A. Weber and E. Ivers-Tiffée, Electrochemical Analysis of Reformate-Fuelled Anode Supported SOFC, J. Electrochem. Soc. 158, pp. B980–B986, 2011.
15. H. Timmermann, W. Sawady, D. Campbell, A. Weber, R. Reimert and E. Ivers-Tiffée, Coke Formation and Degradation in SOFC Operation with a Model reformate from liquid hydrocarbons, J. Electrochem. Soc. 155, pp. B356–B359, 2008.
16. H. Timmermann, D. Fouquet, A. Weber, E. Ivers-Tiffée, U. Hennings and R. Reimert, Internal reforming of methane at Ni/YSZ and Ni/CGO SOFC cermet anodes, Fuel Cells 6, pp. 307–313, 2006.

# Bionotes

**André Weber**
Karlsruhe Institute of Technology (KIT), Institute for Applied Materials (IAM-ET), Adenauerring 20b, 76131 Karlsruhe, Germany
**andre.weber@kit.edu**

André Weber is working as senior scientist (Akademischer Oberrat) at the Institute for Applied Materials – Electrochemical Technologies (IAM-ET) at Karlsruhe Institute of Technology (KIT), Germany. Actually he is heading two groups related to fuel cells and & electrolyzer and battery research. His research is related to the electrical testing and modeling of fuel cells, electrolyzers and batteries, with a special emphasis on the detailed electrochemical characterization by means of impedance spectroscopy. The experimental and theoretical work of his research groups ranges from fundamental studies on model systems to the analysis of commercial products, aiming at a model based understanding of the complex coupling of electrochemical reactions and transport mechanisms within electrochemical devices. He has co-authored several book chapters, and more than 100 peer-reviewed journal papers on scientific topics related to fuel cells and batteries (https://scholar.google.de/citations?hl=de&user=IGECnVQAAAAJ).